ELSEVIER

Journal of Power Sources 104 (2002) 33–39

JOURNAL OF POWER SOURCES

www.elsevier.com/locate/jpowsour

A comparative study on the substitution of divalent, trivalent and tetravalent metal ions in $LiNi_{1-x}M_xO_2$ (M = Cu^{2+}, Al^{3+} and Ti^{4+})

J. Kim*, K. Amine

Electrochemical Technology Program, Argonne National Laboratory, Chemical Technology Division, 9700 South Cass Avenue, Argonne, IL 60439, USA

Received 5 July 2001; accepted 18 July 2001

Abstract

Stabilized lithium nickelate is receiving increased attention as a low-cost alternative to the $LiCoO_2$ cathode now used in lithium batteries. Layered $LiNi_{1-x}M_xO_2$ samples (M = Cu^{2+}, Al^{3+} and Ti^{4+}, where $0.025 \leq x \leq 0.2$) were prepared by solid state reaction at 750 °C under an oxygen stream and subjected to powder X-ray diffraction analysis and coin-cell tests. The Cu^{2+}-substituted samples showed poor structural stability and electrochemical performance, while the Al^{3+}- and Ti^{4+}-substituted samples formed highly ordered and phase-pure layered compounds. Of the three compounds tested, the $LiNi_{1-x}Ti_xO_2$ electrodes exhibited the highest capacity and best electrochemical reversibility. Indeed, the $LiNi_{0.975}Ti_{0.025}O_2$ electrode achieved the highest reversible capacity and energy density (900 Wh/kg) of all known layered $LiNiO_2$ or $LiCoO_2$ electrodes. Indications are that the structural integrity of the $LiNi_{1-x}Ti_xO_2$ materials was preserved because the Ti^{4+} ions prevented impurity Ni^{2+} migration into the lithium sites. The substitution of tetravalent titanium into lithium nickelate has proved to yield promising cathode materials and further studies are needed to optimize electrode composition and processing conditions. Published by Elsevier Science B.V.

Keywords: Lithium nickelate; Lithium battery; Electrochemistry

1. Introduction

Lithium nickelate is considered a promising cathode material for lithium batteries due to its low cost and high energy density. However, the main problem with this material is the difficulty of preparing it in a reproducible way. For example, the actual chemical formula of lithium nickelate is $Li_{1-x}Ni_{1+x}O_2$ ($x > 0$) rather than stoichiometric $LiNiO_2$ [1,2]. Previous crystallographic studies have shown that the x extra nickel ions in $Li_{1-x}Ni_{1+x}O_2$ are located in the lithium plane, hindering smooth transport of lithium ions during electrochemical cycling and resulting in poor performance [3].

In recent years, there has been a great deal of interest in stabilized lithium nickelate. For example, the Co^{3+}-substituted lithium nickelate ($LiNi_{1-x}Co_xO_2$) has phase-pure, two-dimensional structures with good electrochemical properties [4,5]. The use of Co^{3+} substitution originated from the concept of developing a solid solution of $Li_{1-x}Ni_{1+x}O_2$ with isostructural $LiCoO_2$. The resulting material is more stable structurally and electrochemically. Because Co^{3+} substitution for nickel appears to stabilize lithium nickelate, several research groups have investigated trivalent metal substitutions such as Al^{3+}, Mn^{3+}, Ti^{3+} or an equal amount of Ti^{4+} and Mg^{2+}, to attain structural or safety improvements [6–9]. All of these substitutions have one common feature: they strictly manage and maintain the oxidation state of the substituted metal ions around 3+, so that no unexpected structural interference occurs.

Recently, we investigated Ti^{4+} substitution and this material has also proven to be promising [10]. In this paper, we report the results from the synthesis and testing of Cu^{2+}-, Al^{3+}- and Ti^{4+}-substituted lithium nickelate as the cathode in lithium batteries. The objective was to obtain a better understanding of the effect of the oxidation state of the substituent. Since titanium is not electrochemically active around the 4 V region, where $Ni^{3+/4+}$ and $Co^{3+/4+}$ electrochemical couples are activated, we chose to study Al^{3+} instead of Co^{3+}.

2. Experimental

The $LiNi_{1-x}M_xO_2$ (M = Cu^{2+}, Co^{3+} and Ti^{4+}, where $0.025 \leq x \leq 0.2$) materials were synthesized by a solid state

* Corresponding author. Tel.: +1-630-252-6772; fax: +1-630-252-4176.
E-mail address: kimj@cmt.anl.gov (J. Kim).

0378-7753/02/$ – see front matter. Published by Elsevier Science B.V.
PII: S0378-7753(01)00900-4

reaction involving LiOH, $Ni(OH)_2$ and either $Cu(OH)_2$, $Al(OH)_3$ or TiO_2 (anatase) powders. The required amounts of raw material powders were ball-milled for 24 h. The solid state reaction proceeded at 750 °C under an oxygen or air stream for 30 h. The samples were characterized by powder X-ray diffraction and the lattice parameters were derived using the Rietveld method.

The electrochemical performance of $LiNi_{1-x}M_xO_2$ electrodes was determined in galvanostatic cycling experiments. Coin-type cells with the different cathode materials were

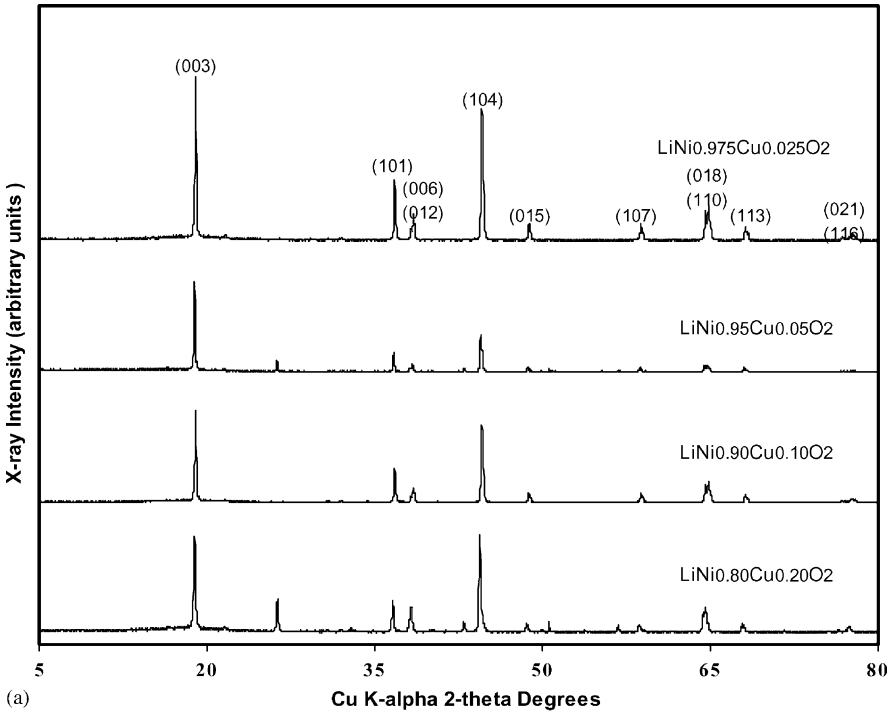

(a)

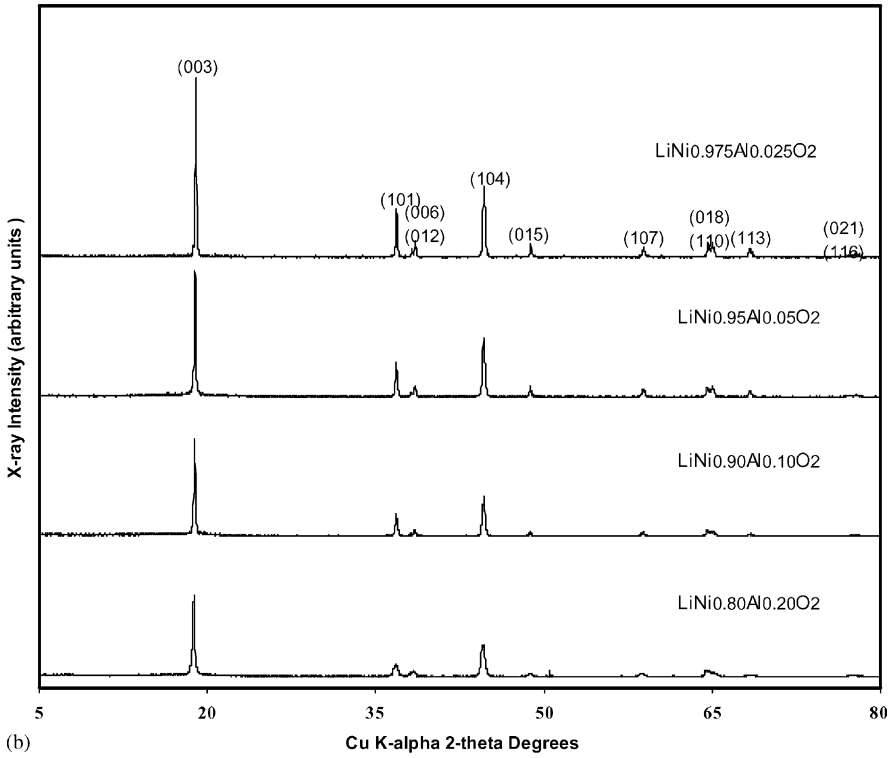

(b)

Fig. 1. X-ray powder diffraction patterns of (a) $LiNi_{1-x}Cu_xO_2$; (b) $LiNi_{1-x}Al_xO_2$ and (c) $LiNi_{1-x}Ti_xO_2$ ($0.025 \leq x \leq 0.2$) obtained by solid state reaction at 750 °C for 30 h.

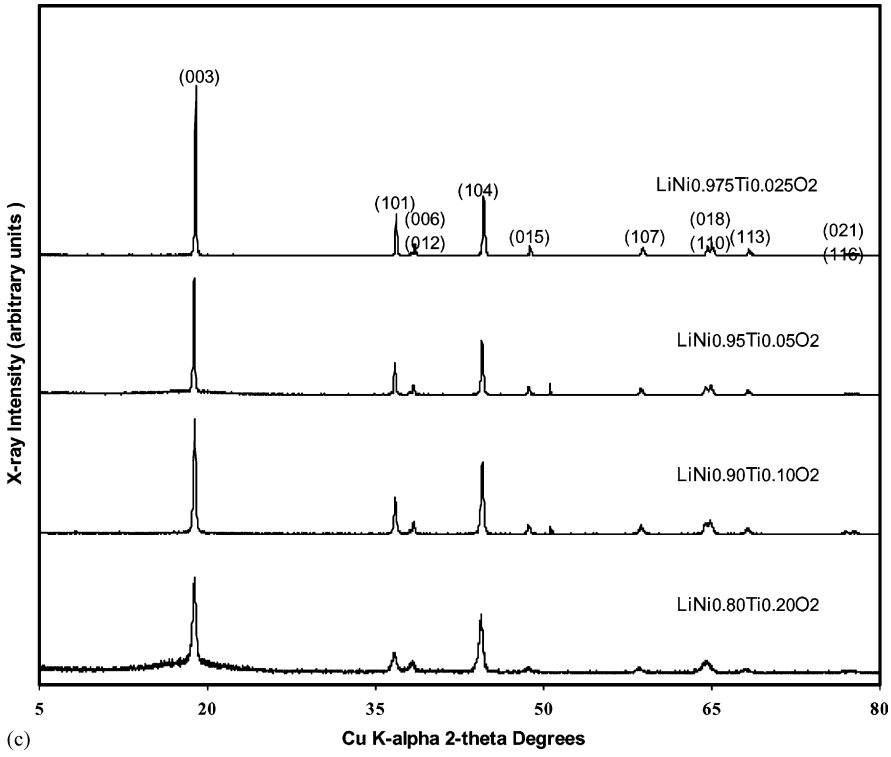

Fig. 1. (*Continued*).

prepared inside a dry room. The electrolyte consisted of 1 M $LiPF_6$ with ethylene carbonate and diethyl carbonate (1:1). The $LiNi_{1-x}M_xO_2$ powders were mixed with 20% carbon and 10% PVDF binder in 1-methyl-2-pyrrodinone solvent. The resulting paste was cast on an aluminum foil. The working electrodes had 1.6 cm^2 geometric areas. Cells were tested in the voltage range 4.3–2.8 V with a current density of 0.2 mA/cm^2.

3. Results and discussion

3.1. Formation of $LiNi_{1-x}M_xO_2$ solid solutions

As shown in Fig. 1, X-ray diffraction patterns of the samples obtained by a solid state reaction involving LiOH, $Ni(OH)_2$ and either $Cu(OH)_2$, $Al(OH)_3$ or TiO_2 at 750 °C represent phase-pure layered structures. However, compared to the samples of $LiNi_{1-x}Al_xO_2$ and $LiNi_{1-x}Ti_xO_2$, the $LiNi_{1-x}Cu_xO_2$ samples had a very low Bragg intensity ratio $R_{(003)} = I_{(003)}/I_{(1\,0\,4)}$, which can serve as a measure for the stoichiometry and degree of order in the $LiNiO_2$ system. As the amount of Cu^{2+} increased (e.g. $LiNi_{0.8}Cu_{0.2}O_2$), the Bragg intensity ratio became negative. We reached one conclusion from the results in Fig. 1(a). First, the materials with large amounts of Cu^{2+} have a rock salt structure rather than a rhombohedral layered (space group: $R\bar{3}m$) structure. In other words, the materials have a cubic lattice formation because there is no preferred occupation of the 3*a* and 3*b* sites by transition metal ions (nickel and copper in this case) and lithium ions in an oxygen close-packed framework.

By contrast, the samples with Al^{3+} and Ti^{4+} ions have a phase-pure layered structure. Since $LiAlO_2$ is isostructural with $LiNiO_2$, the $LiNi_{1-x}Al_xO_2$ solid solution formed a pure layered structure without any detectable impurities in the X-ray diffraction pattern, as shown in Fig. 1(b). However, the mismatch of aluminum and nickel ions may cause lattice strain and the $LiNi_{1-x}Al_xO_2$ samples with larger amounts of aluminum have much broader peaks. This finding suggests that the increased aluminum substitution (e.g. from $LiNi_{0.9}Al_{0.1}O_2$ to $LiNi_{0.8}Al_{0.2}O_2$) leads to inferior electrochemical performance, although the aluminum substitution does have beneficial effects, such as safety improvement.

Similar to the $LiNi_{1-x}Al_xO_2$ samples, the X-ray diffraction patterns of the $LiNi_{1-x}Ti_xO_2$ samples represent a phase-pure, layered structure, as indicated by the data in Fig. 1(c).

Fig. 2(a) and (b) show the variations in the hexagonal cell parameters (*a* and *c*) versus *x* in $LiNi_{1-x}M_xO_2$ ($M = Cu^{2+}$, Al^{3+} and Ti^{4+}). The $LiNi_{1-x}Cu_xO_2$ has a relatively low degree of trigonal distortion (*c*/*a*), which sharply drops with increasing copper content (Fig. 2(c)), indicating that this material's structure becomes totally disordered. On the other hand, the aluminum- and titanium-substituted samples have similar trigonal distortion (*c*/*a*) values without noticeable structural disorder. For the aluminum-substituted samples, the average metal–metal intra-sheet distance (a_{hex}) decreased and the lattice parameter *c* increased as the aluminum amount increased. However, as the amount of

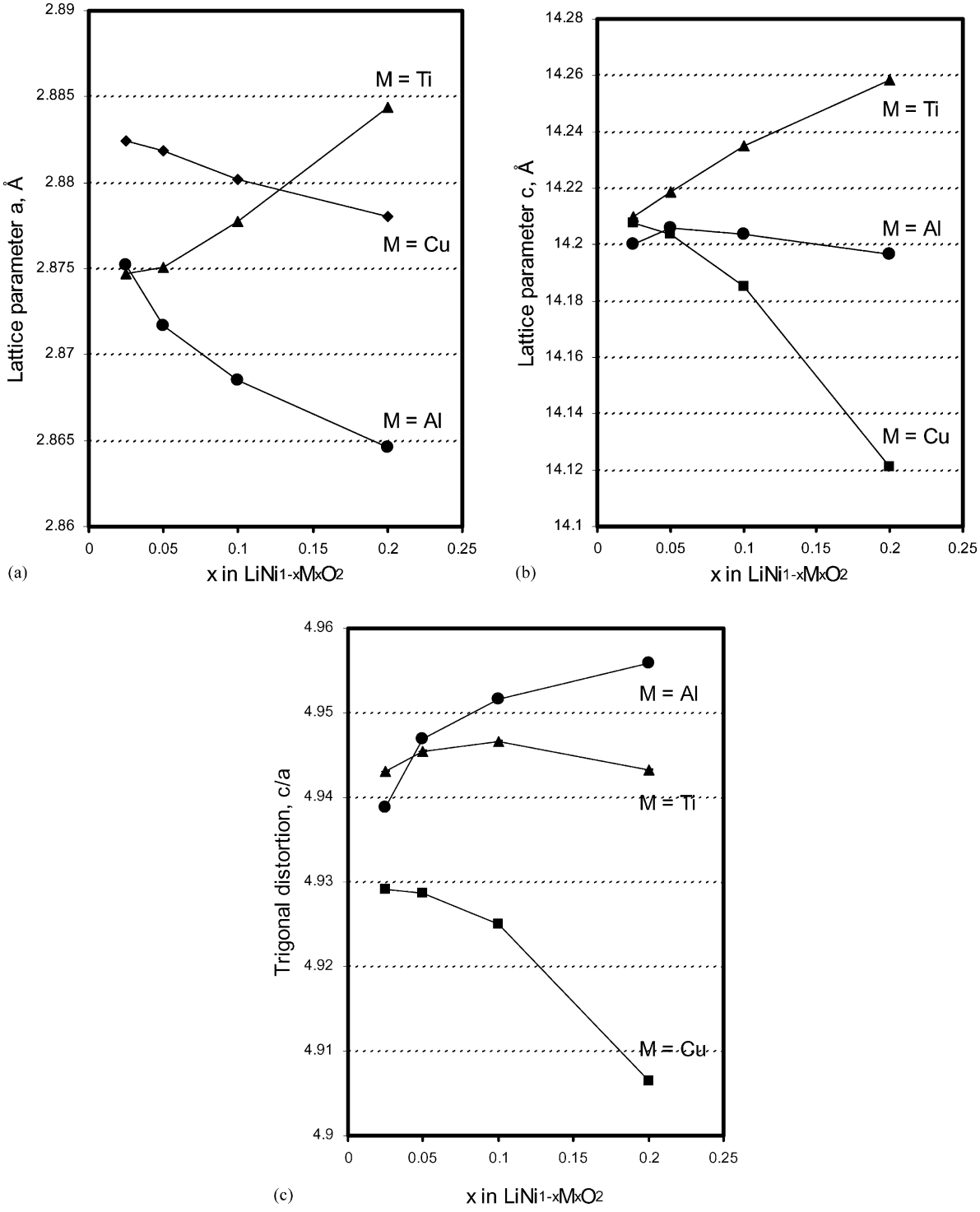

Fig. 2. (a) Hexagonal lattice parameter a (intra-sheet distance); (b) hexagonal lattice parameter c, which is equal to three times the average interlayer distance and (c) trigonal distortion of $LiNi_{1-x}M_xO_2$ ($M = Cu^{2+}$, Al^{3+} and Ti^{4+}).

titanium increased in the $LiNi_{1-x}Ti_xO_2$ samples, a_{hex} increased. In general, the average metal–metal interlayer distance ($c_{hex}/3$) also increased due to the relatively strong electrical repulsion between layers caused by Ti^{4+} substitution. The Ti^{4+} ions appear to have different local ionic ordering compared with Ni^{3+} ions and tend to form more ionic $(Ni_{1-x}Ti_xO_2)_n$ sheets, which yield high c/a values, although axis-a (intra-sheet distance) enlarges simultaneously. The degree of trigonal distortion reflects typical c/a values of hexagonal-close-packed structures, 4.94–4.95. These c/a values differ somewhat compared with those from our previous report [10]. This discrepancy is probably due to

the different amounts of lithium in the synthesized solid solutions, since we used an excess lithium method in the earlier experiment.

3.2. Electrochemical studies of $LiNi_{1-x}M_xO_2$ solid solutions

Electrochemical studies were carried out to compare the effect on performance of the different oxidation states of the substituents in the $LiNiO_2$ system. The charge and discharge curves of the cells in the first cycle are given in Figs. 3–5. The $LiNi_{1-x}Cu_xO_2$ electrode as shown in Fig. 3 showed very severe capacity reduction in the first cycle compared with the $LiNi_{1-x}Al_xO_2$ and $LiNi_{1-x}Ti_xO_2$ electrodes Which are shown in Figs. 4 and 5, respectively. Even very small amounts of Cu^{2+} substitution (e.g. 2.5%) seem to cause serious structural problems. This finding suggests that Cu^{2+}not only works as an inactive mass, but also hinders the lithium insertion and extraction by disturbing the structural integrity of layered $LiNiO_2$ materials. The capacity data for a $LiNi_{1-x}Cu_xO_2$ electrode operated for 100 cycles are also shown in Fig. 3. The cell was cycled with a current density of 0.2 mA/cm^2 (corresponding to about the *C*/5 rate) between cut-off voltages of 2.8 and 4.3 V. As anticipated from the low capacities due to structural problems, the capacity retention of $LiNi_{1-x}Cu_xO_2$ with continued cycling is very poor. In the case of 20% Cu^{2+} substitution, the discharge capacity faded extremely rapidly. We believe that these materials have not only nickel ions in the lithium sites, but also Cu^{2+} ions that hinder lithium insertion/extraction and drastically degrade electrochemical performance.

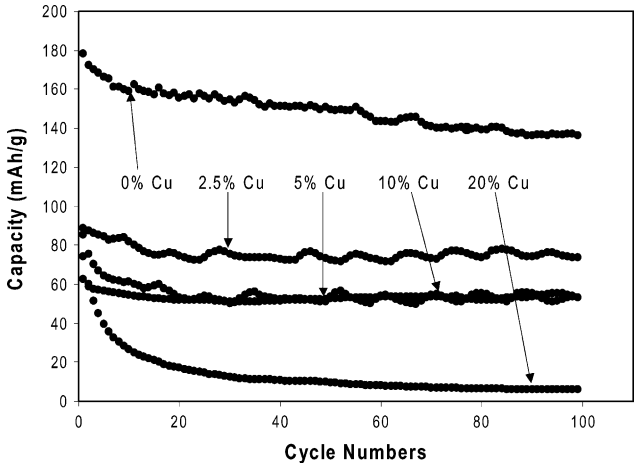

Fig. 3. Galvanostatic cycling results for capacity retention of $LiNi_{1-x}Cu_xO_2$ ($0.025 \leq x \leq 0.2$) samples. The data were recorded with a current density of 0.2 mA/cm^2.

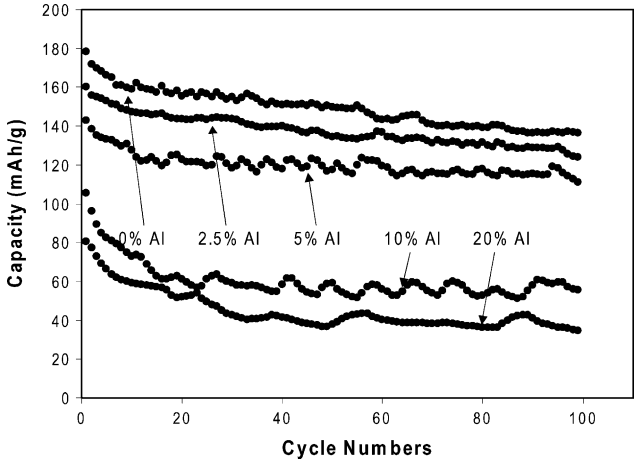

Fig. 4. Galvanostatic cycling results for capacity retention of $LiNi_{1-x}Al_xO_2$ ($0.025 \leq x \leq 0.2$) samples. The data were recorded with a current density of 0.2 mA/cm^2.

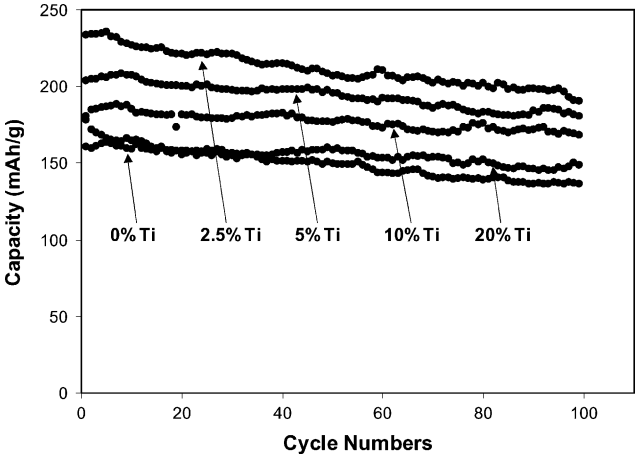

Fig. 5. Galvanostatic cycling results for capacity retention of $LiNi_{1-x}Ti_xO_2$ ($0.025 \leq x \leq 0.2$) samples. The data were recorded with a current density of 0.2 mA/cm^2.

The Fig. 4 presents the electrochemical performances of the $LiNi_{1-x}Al_xO_2$ electrode. The capacity decreases as aluminum content increases, which is to be expected given that aluminum is not electrochemically active. However, the discharge capacities for materials with more than 10% Al^{3+} show a rapid decline, indicating that the lithium insertion proceeds irreversibly. This problem is probably caused by a partial structural instability that occurs while the $LiNi_{1-x}Al_xO_2$ electrode is charged. Although the aluminum substitution favors and maintains the layered structure by forming a $LiNi_{1-x}Al_xO_2$ solid solution with the same structure ($R\bar{3}m$) as $LiNiO_2$ and a-$LiAlO_2$, the local distortion [11] of aluminum by movement along the trigonal symmetric axis causes this material to lose its preferred occupation of 3*a* octahedral sites and leads to partial pseudo-tetrahedral coordination. Also, we suspect that the formation of an aluminum-rich insulating phase at the fully charged state (e.g. $Li_{0.1}Ni_{1-x}Al_xO_2$) might harm the charge–discharge reversibility, although it is beneficial to overcharge protection. As expected, the materials with >10% aluminum had poor capacity retention. These results suggest that the threshold concentration for aluminum substitution lies between 5 and 10%.

Compared with the Cu^{2+}- and Al^{3+}-substituted materials, the $LiNi_{1-x}Ti_xO_2$ electrode shows superior electrochemical

performance (Fig. 5). Since Ti^{4+} is not electrochemically active in the voltage range of 4.3–2.8 V, the capacity decreases almost linearly as the titanium content increases. However, the 10 and 20% titanium samples show better cyclability, although they have lower capacities than the 2.5 and 5% titanium samples (187 and 161 mAh/g compared to 235 and 207 mAh/g, respectively). In fact, the 10% titanium sample had the same discharge capacity as pure $LiNiO_2$, both of which have the same amount of electrochemically inactive ions.

Overall, the $LiNi_{1-x}Ti_xO_2$ $(0.025 \leq x \leq 0.2)$ samples exhibit excellent capacity retention over 100 cycles. The electrochemical performance is superior to that found with the Cu^{2+} and Al^{3+} materials. The Ti^{4+} substitution led to a rigid electrode structure and excellent electrochemical performance. We assume that the overall good electrochemical performance of $LiNi_{1-x}Ti_xO_2$ arises from the prevention of the migration of impurity Ni^{2+} ions into the lithium plane as a result of the Ti^{4+} substitution. In addition, samples containing the higher titanium amounts undergo a one-phase instead of two-phase oxidation/reduction reaction, as we reported earlier [10], which leads to improved capacity retention under extended cycling. Also worth noting is that the $LiNi_{1-x}Ti_xO_2$ is a less expensive and more environmentally friendly electrode material than the cobalt-containing electrode.

3.3. Structural stability of $LiNi_{1-x}M_xO_2$ solid solutions

Fig. 6 presents a schematic illustration (not crystallographic) of the structural stability of $LiNi_{1-x}M_xO_2$ (M = Cu^{2+}, Al^{3+} and Ti^{4+}). For convenience, the oxygen ions are represented as a half of oxygen, in other words, one negatively charged object. As we discussed earlier, because of the difficulty in synthesizing stoichiometric $LiNiO_2$, it is typically formed as a disordered $Li_{1-x}Ni_{1+x}O_2$. Our crystallographic studies suggest that the excess nickel ions in $Li_{1-x}Ni_{1+x}O_2$ are positioned in the lithium plane and hinder the smooth transport of lithium ions through that plane. Divalent copper ions act similarly to impurity nickel ions, as mentioned above. Therefore, their substitution in the lithium nickelate may damage the structural integrity even more, as indicated by Fig. 6(a). This conclusion is supported by the fact that the Bragg intensity is very low, even negative in the case of 20% copper substitution, and the *c/a* ratio decreases as the copper content increases. As a result, $LiNi_{1-x}Cu_xO_2$ has very poor electrochemical performance.

Since $LiAlO_2$ and $LiNiO_2$ are isostructural, $LiNi_{1-x}Al_xO_2$ is a structurally and electrochemically stable phase. However, even after substitution of Ni by Al^{3+}, Ni^{2+} ions may form as long as the material has been exposed to high firing temperatures or electrochemical cycling. The chemical formula of $LiNi_{1-x}Al_xO_2$ can be written more accurately as $LiNi_{1-x}Al_xO_{2-y}$ and the average oxidation state of transition metal ions is lower than 3+. As shown in Fig. 6(b), some portion of the lithium ions will be decomposed and separated from the solid structure, and impurity Ni^{2+} ions may migrate to lithium sites under extended cycling.

By contrast, Ti^{4+} substitution compensates the electronic charge deficit and structural instability due to Ni^{2+}, as conjectured schematically in Fig. 6(c). In $LiNi_{1-x}Ti_xO_2$, the transition metal layer appears to contain Ni^{3+}, Ti^{4+} and minor Ni^{2+}. This material can maintain an impurity-free

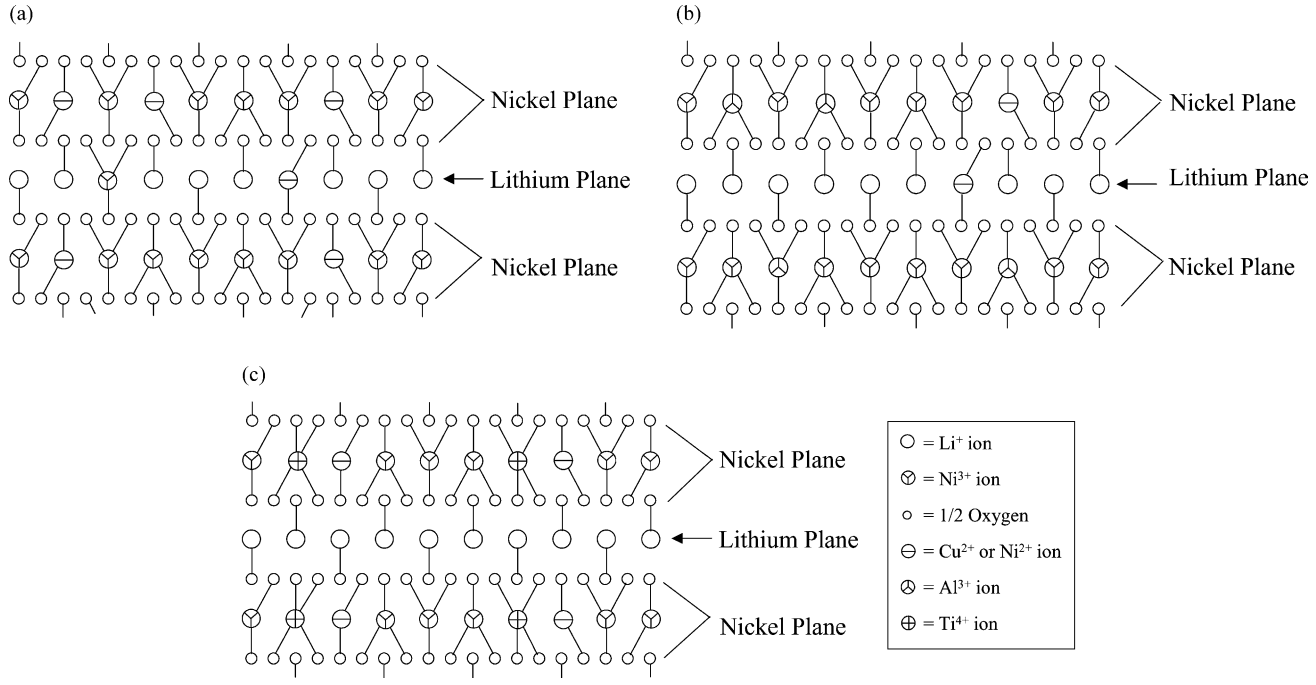

Fig. 6. Schematic illustration of the structural stability of (a) $LiNi_{1-x}Cu_xO_2$; (b) $LiNi_{1-x}Al_xO_2$ and (c) $LiNi_{1-x}Ti_xO_2$. The oxygen ions are represented as one half oxygen of one negatively charged object.

lithium plane thereby, facilitating smooth lithium transport. As can be seen in Fig. 5, the capacity of $LiNi_{1-x}Ti_xO_2$ increases at initial cycling, suggesting that Ti^{4+} ions somehow act as a buffer to the generation of impurity Ni^{2+} ions during cycling. The Ti^{4+} may simultaneously compensate for the charge deficit caused by Ni^{2+} ions in the transition metal layer and prohibit Ni^{2+} migration into the lithium layer. Therefore, the Ti^{4+} substitution could maintain overall electronic neutrality and structural integrity.

4. Conclusions

We have investigated the synthesis and electrochemical performance of $LiNi_{1-x}M_xO_2$ ($M = Cu^{2+}$, Al^{3+} and Ti^{4+} where $0.025 \leq x \leq 0.2$) as an alternative cathode material for lithium batteries. The results showed that $LiNi_{1-x}Cu_xO_2$ has poor structural stability and electrochemical performance. While structurally stable, $LiNi_{1-x}Al_xO_2$ materials with high aluminum content exhibit poor capacity retention with cycling, probably due to lattice strain by mismatch of Al and Ni ions. The $LiNi_{1-x}Ti_xO_2$ electrodes exhibit high capacity with excellent electrochemical cyclability. Among these electrodes, $LiNi_{0.975}Ti_{0.025}O_2$ attained the highest reversible capacity and energy density (900 Wh/kg) of all known layered $LiNiO_2$ or $LiCoO_2$ materials. Further studies are needed on the optimization of the electrode composition and processing conditions and are being carried out for high power and high energy applications, such as electric vehicle propulsion. Also, we are performing a more careful crystallographic study by means of other diffraction techniques such as neutron diffraction.

Acknowledgements

The authors acknowledge the financial support of the Office of Advanced Transportation Technology, US Department of Energy, under Contract number W-31-109-ENG-38.

References

[1] J.B. Goodenough, D.G. Wickman, W.J. Croft, J. Phys. Chem. Solid 5 (1958) 107.
[2] V.W. Bronger, H. Bade, W. Klemm, Z. Anorg. Allg. Chem. 333 (1964) 188.
[3] W. Li, J.N. Reimers, J.R. Dahn, Solid State Ionics 67 (1993) 123.
[4] C. Delmas, I. Saadoune, Solid State Ionics 53–56 (1992) 370.
[5] E. Zhecheva, R. Stoyanova, Solid State Ionics 66 (1993) 149.
[6] Q. Zhong, U. von Sacken, J. Power Sources 54 (1995) 221.
[7] E. Rossen, C.D.W. Jones, J.R. Dahn, Solid State Ionics 57 (1992) 311.
[8] H. Arai, S. Okada, Y. Sakurai, J. Yamaki, J. Electrochem. Soc. 144 (1997) 3117.
[9] Y. Gao, M.V. Yakovleva, W.B. Ebner, Electrochem. Solid State Lett. 1 (1998) 117.
[10] J. Kim, K. Amine, Electrochem. Commun. 3 (2001) 52.
[11] R. Stoyanova, E. Zhecheva, E. Kuzmanova, R. Alcantara, P. Lavela, J.L. Tirado, Solid State Ionics 128 (2000) 1.